

Common exchange-biased spin switching mechanism in orthoferrites

I. Fita,^{1,*} A. Wisniewski,¹ R. Puzniak,¹ E. E. Zubov,² V. Markovich,³ and G. Gorodetsky³

¹*Institute of Physics, Polish Academy of Sciences, Aleja Lotnikow 32/46, PL-02668 Warsaw, Poland*

²*G. V. Kurdyumov Institute for Metal Physics, NASU, 03680 Kyiv, Acad. Vernadsky Boulevard 36, Ukraine and Vasyl' Stus Donetsk National University, 021021, Vinnytsia, Ukraine*

³*Department of Physics, Ben-Gurion University of the Negev, P.O. Box 653, 84105 Beer-Sheva, Israel*



(Received 28 May 2018; revised manuscript received 8 July 2018; published 21 September 2018)

The unconventional exchange-bias (EB) effect in single crystals of $R\text{FeO}_3$ ($R = \text{Nd}, \text{Sm}$) compensated ferrimagnets (fMs), composed of two antiferromagnetically (AFM) coupled R and Fe sublattices with opposite ferromagnetic (FM) moments, exhibiting the FM moment reversal via a fast spin switching is reported. In NdFeO_3 , the EB anisotropy field emerges and diverges upon approaching the compensation temperature $T_{\text{comp}}^{\text{Nd}} = 9.2$ K, and changes sign with crossing $T_{\text{comp}}^{\text{Nd}}$, in similarity to the behavior observed recently in ErFeO_3 . In contrast, SmFeO_3 exhibits a substantial EB, not only at its $T_{\text{comp}}^{\text{Sm}} = 4.8$ K, but also at higher temperatures up to 100 K, and the EB changes its sign with increasing cooling field. It is shown that in all known $R\text{FeO}_3$ ($R = \text{Nd}, \text{Sm}, \text{Er}$) compensated fMs the field-induced FM moment reversal is similarly exchange biased near T_{comp} .

DOI: [10.1103/PhysRevB.98.094421](https://doi.org/10.1103/PhysRevB.98.094421)

I. INTRODUCTION

Ferrimagnetic (fM) orthoferrites of $R\text{FeO}_3$, where R is a rare-earth ion, have been revisited in the last years because of their attractiveness for practical applications, such as ultrafast spin switching, spin-reorientation transition, field- and temperature-induced sharp magnetization reversal (MRev), and multiferroicity [1–4]. In these compounds, the weak ferromagnetic (FM) moment results from the canted antiferromagnetic (AFM) ordering of Fe spins below $T_N \approx 700$ K due to the Dzyaloshinskii-Moriya (DM) interactions, while the opposite compensating paramagnetic moment of R spins appears owing to a strong AFM coupling between $4f$ and $3d$ ions within the unit cell. Due to this mechanism, the Er, Nd, and Sm orthoferrites exhibit a specific compensation temperature T_{comp} at which the two opposite moments cancel each other so that the net magnetization vanishes, and below T_{comp} the FM moment is aligned oppositely to the moderate applied magnetic field, demonstrating a negative magnetization. The first-principles calculations confirmed such a scenario in NdFeO_3 [5].

Three types of competitive exchange interactions between magnetic ions, Fe-Fe, R -Fe, and R - R , determine the magnetic phenomena in Er, Nd, and Sm orthoferrites having the same $Pbnm$ orthorhombic structure. The strong Fe-Fe exchange is responsible for the noncollinear AFM ordering of Fe spins at temperatures ~ 700 K, while the weak R - R interactions lead to the AFM order in R sublattice at much lower temperatures of ~ 1 K. The anisotropic R -Fe exchange is known to induce in orthoferrites the Fe spin reorientation (SR), leading to the

weak FM moment rotation from the c axis to the a axis. The temperature of the reorientation T_{SR} varies in a wide range because the R -Fe interaction differs significantly in various compounds. As follows, SmFeO_3 with the strongest R -Fe interaction exhibits a SR transition at temperature $T_{\text{SR}} \approx 480$ K, while in both Nd and Er orthoferrites a transition occurs at around 100 K [3–5]. Moreover, SmFeO_3 demonstrates more complex fM structure and distinct magnetic behavior among other orthoferrites due to the presence of two nonequivalent canted AFM Fe spin pairs [3,6].

Currently, great interest is being paid to the compensated fM materials exhibiting, together with exotic MRev and negative magnetization phenomena, the exchange-bias (EB) effect [7–10]. The ordinary EB, discovered by Meiklejohn and Bean (Ref. [11]), represents a shift in magnetization hysteresis loop from the origin, emerging at the interface between strongly anisotropic AFM and soft FM phases due to the exchange interaction [12]. However, this behavior is not limited to the system with AFM-FM interface interactions since the exchange coupled fM-AFM systems may have essentially the same properties. The intriguing possibility of the compensated fM material to cause the exchange-biased hysteresis loops was pointed by Meiklejohn (Ref. [13]) already in 1962. An interesting example revealing how EB at a compensated fM interface may occur has been described in Ref. [14]. In addition, the DM interactions, which play a crucial role in the magnetism of orthoferrites, were recently found to be essential for the possible mechanisms of EB in fMs [15,16]. The origin of the EB effect found in single-phase fMs [7,9,10] near T_{comp} appears to be very different from that of traditional interfacial EB, and it rather links to the intrinsic exchange coupling between opposing spins inside the unit cell. It has been proposed by Webb *et al.* (Ref. [17]) that the EB anisotropy inversely proportional to the net FM moment, $H_{\text{EB}} \sim (M_A - M_B)^{-1}$, occurs at the T_{comp} of fM comprising two AFM coupled

*Corresponding author: Institute of Physics, Polish Academy of Sciences, Aleja Lotnikow 32/46, PL-02-668 Warsaw, Poland; ifita@ifpan.edu.pl

sublattices A and B with opposite FM moments M_A and M_B . This model well illustrates the unique exchange-biased FM moment reversal recently observed in single-crystalline ErFeO_3 [9]. Namely, the EB field diverges and changes sign at T_{comp} when the net FM moment approaches zero and changes its direction to the opposite one with crossing T_{comp} . Remarkably, the EB is negative or positive when the FM moment and an applied small magnetic field are parallel or antiparallel, respectively. The last spin configuration happens in the case of a metastable state exhibiting a negative magnetization. Moreover, the EB sign could be inverted by using a special cooling-field procedure. This exceptional feature is the motivation for further EB studies in other orthoferrites exhibiting a magnetic compensation. In this paper, we show that the FM moment reversal, happening in a way of fast spin switching over 180° , is similarly exchange biased around the T_{comp} in all known compensated orthoferrites of $R\text{FeO}_3$ ($R = \text{Nd}, \text{Sm}, \text{Er}$), despite their very different compensation and spin-reorientation temperatures. Moreover, in SmFeO_3 , representing a complicated AFM order caused by nonequivalent spins, the EB was found also at temperatures far above $T_{\text{comp}}^{\text{Sm}} = 4.8 \text{ K}$ and its sign alters from the negative to the positive one with increasing cooling field.

II. RESULTS AND DISCUSSION

Magnetization measurements were performed on NdFeO_3 and SmFeO_3 single crystals with sizes of $2.4 \times 2.2 \times 2.0$ and $3.3 \times 2.2 \times 1.2 \text{ mm}^3$, respectively, grown by a flux method at the Weizmann Institute [18], in the temperature range 3–300 K and in a magnetic field up to 15 kOe, using a PAR (Model 4500) vibrating sample magnetometer. The magnetization loops presented in Fig. 1(a) show that the FM moment of NdFeO_3 at 300 K aligns along the c axis in accordance with the $\Gamma_4[Gx Fz]$ spin configuration in Bertaut's notation. In contrast, the FM moment of SmFeO_3 is aligned along the a axis (the $\Gamma_2[Fx Gz]$ phase), because in this crystal the Γ_4 to Γ_2 spin reorientation occurs at temperatures of $\sim 480 \text{ K}$ [3]. In NdFeO_3 , such SR transition occurs at lower temperatures [5], as it is evidenced in Fig. 1(c) by the temperature dependences of magnetization measured at 100 Oe upon field cooling (FC mode) along both the a and c axes. Namely, the Fe spins rotate continuously from Γ_4 to the Γ_2 configuration in temperature intervals between 182 and 102 K, marked by the shadow area in Fig. 1(c). With further cooling below 100 K, both fMs preserve the Γ_2 phase, whereas a noticeable paramagnetic moment of R spins, induced by the AFM R -Fe exchange interaction and oriented antiparallel to the FM moment of Fe spins produced by the DM interaction, increases according the Curie-Weiss law. At small applied field, this mechanism leads to a compensation of the net spontaneous FM moment along the a axis at temperatures $T_{\text{comp}} = 9.2$ and 4.8 K in Nd and Sm compounds, respectively [see Figs. 1(c) and 1(b) and insets therein]. Below T_{comp} , the induced R spin moment dominates over the Fe one, and therefore the net FM moment appears to orientate oppositely to the applied field, indicating a metastable state with negative magnetization ($M < 0$), which signifies the first-order magnetic transition at T_{comp} . The same $M < 0$ state appears similarly at $T > T_{\text{comp}}$ during the reverse warming process (FW mode), performed in the

following manner: (1) after FC, at a temperature of 3 K, the negative net FM moment was inverted over 180° by applying a field of 10 kOe and restoring in this way the equilibrium $M > 0$ state (the magnetization and field vectors are parallel); (2) subsequently, a small magnetic field was renewed and the FW M vs T curve was recorded on warming, see Figs. 1(c) and 1(b). For NdFeO_3 , the very similar M vs T curves were also obtained when measured with the zero-field-cooling (ZFC) mode, see Fig. 1(d). With increasing T the antiparallel R and Fe moments cancel each other at T_{comp} , and above T_{comp} the state with negative magnetization develops again because now the prevalent Fe moment points oppositely to the magnetic field. Note that the temperature of intersecting both FC and FW curves, which is not dependent on the measuring field magnitude, is the true value of T_{comp} . With further increasing T , the magnetization reaches its saturated negative value, due to the vanishing of the positive contribution from R spins, and then it suddenly switches to the positive value at a spin switching temperature T_{ssw} . [See the possible spin configurations at temperatures below and above T_{ssw} in Fig. 1(d).] This spin switching is actually the spontaneous spin reversal over 180° , indicated by vertical arrows in Figs. 1(c) and 1(d), and T_{ssw} depends strongly on applied magnetic field. [See T_{ssw} vs H dependences in the inset of Fig. 1(d).] This fascinating unusual phenomenon has been recently studied in both SmFeO_3 (Ref. [4]) and NdFeO_3 (Ref. [5]) single crystals, where the spontaneous reversal of the FM moment of Fe at T_{ssw} was interpreted as a first-order spin-flip transition. Very similar spin switching leading to a sign change of the magnetization has been observed in other fMs, such as $\text{Fe}_2\text{F}/\text{Ni}$ heterostructures. It was suggested that this transition is caused by the FM Zeeman energy overcoming the interfacial AFM coupling [19,20]. It is seen in Fig. 1 that, at small applied field the T_{ssw} vs H dependence differs significantly for Nd and Sm compounds, most likely because of different R -Fe AFM interaction. Namely, the temperature region of existence of the metastable state with negative magnetization $\Delta T = T_{\text{ssw}} - T_{\text{comp}}$ becomes larger in the crystal with stronger R -Fe coupling. Hence, SmFeO_3 with the strongest among the orthoferrites AFM coupling between R and Fe spins [3,4,6] shows at applied field of 100 Oe an unchanging negative magnetization up to temperatures higher than 350 K, i.e., ΔT is extremely large (see Fig. 1(b) and Ref. [3]). At the same applied field, NdFeO_3 shows the spin switching transition at $T_{\text{ssw}} \approx 50 \text{ K}$, i.e., $\Delta T \approx 40 \text{ K}$, and ErFeO_3 (Ref. [9]) shows $T_{\text{ssw}} \approx 55 \text{ K}$ and a narrower region of metastable state $\Delta T \approx 10 \text{ K}$. Summarizing, all studied $R\text{FeO}_3$ compensated fMs reveal the very analogous “butterfly” behavior of the a axis magnetization, indicative of the first-order transition at T_{comp} , representing the metastable states with negative magnetization and the temperature-driven FM moment reversal over 180° to the direction of applied magnetic field.

Figure 2 shows the central parts of the magnetization hysteresis $M(H)$ loops of NdFeO_3 crystal at several temperatures near T_{comp} measured in the direction of the a axis between $\pm 15 \text{ kOe}$ and with a cooling field of 15 kOe applied at 300 K. In a simple approximation, the $M(H)$ loop of compensated fM may be considered as a sum of two contributions, each of which can be interpreted separately. The first one is a linear field-dependent AFM contribution, $\chi_{\text{HF}} H$, where

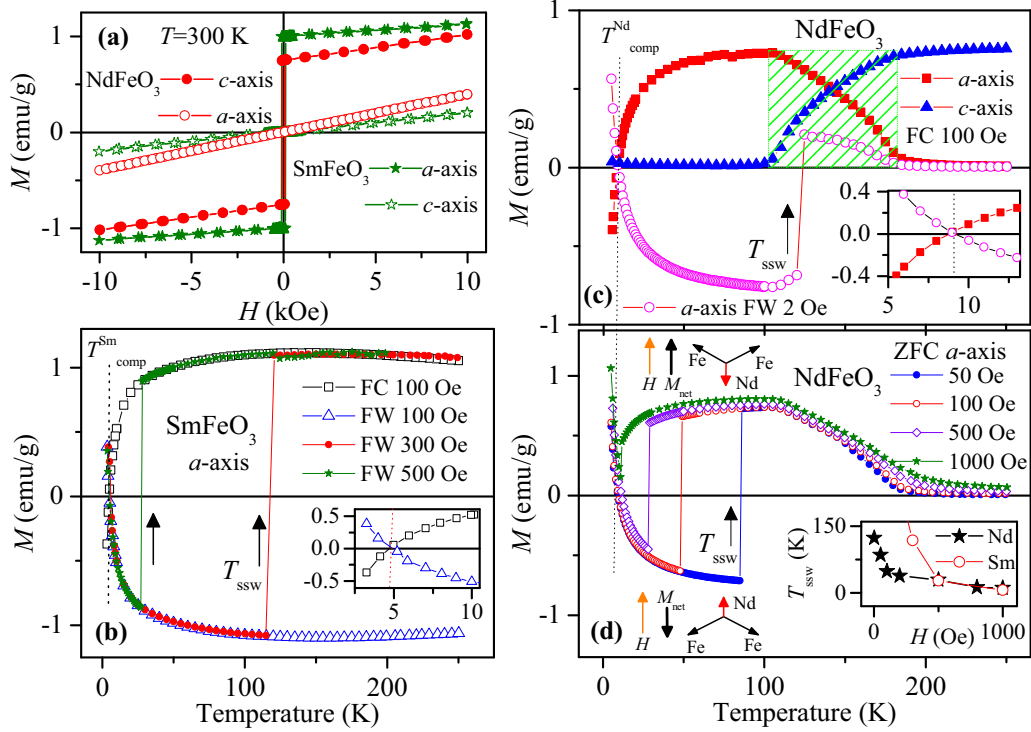


FIG. 1. (a) Magnetization hysteresis loops of NdFeO₃ and SmFeO₃ single crystals, measured along both the *c* and *a* axes at 300 K. (b) Temperature dependence of magnetization of SmFeO₃ single crystal measured along the *a* axis upon cooling (FC) at 100 Oe and on warming (FW) at several applied fields. The inset shows the sign change in magnetization at the compensation point $T_{\text{comp}}^{\text{Sm}} = 4.8$ K. (c) Magnetization of NdFeO₃ measured with FC mode along both the *a* and *c* axes at 100 Oe, and with FW mode at $H = 2$ Oe after cooling at 10 kOe. The shadow marks the area of the Fe spin reorientation. The inset shows the sign change in magnetization at $T_{\text{comp}}^{\text{Nd}} = 9.2$ K. (d) ZFC magnetization of NdFeO₃ measured along the *a* axis on warming at several applied fields. The possible spin configurations below and above the spin switching temperature T_{ssw} are shown. The inset presents the T_{ssw} vs H dependence in both Nd and Sm compounds.

$\chi_{\text{HF}} = dM/dH$ is the constant $M(H)$ slope at high fields, which is shown in Figs. 2(a) and 2(b) as a dashed line through the origin. The second component of the loop arises from the field-dependent weak FM moment due to the canted AFM structure $M_{\text{FM}}(H)$, which exhibits abrupt reversals via the 180° domain wall motion [21] at switching fields H_1 and H_2 . The $M_{\text{FM}}(H)$ curves, shown in Fig. 2 by solid lines as square loops, are calculated by extracting the AFM contribution from the original $M(H)$ loops in accordance with above approximation: $M(H) = \chi_{\text{HF}}H + M_{\text{FM}}(H)$. Note that this simple picture was exploited previously by Webb *et al.* (Ref. [22]) to identify the true coercive field of the compensated fMs near T_{comp} . Indeed, it is easy to see in Figs. 2(c) and 2(d) that fields H_1 and H_2 , at which the FM moment reverses to the opposite direction, are the true coercive fields, but not the fields at which the net magnetization becomes zero.

The rectangular $M(H)$ loops of NdFeO₃ at temperatures relatively far from T_{comp} are quite symmetric, signifying the absence of an exchange-bias effect, see Fig. 2. As the temperature approaches $T_{\text{comp}} = 9.2$ K, the narrow loop drastically changes its form (see Fig. 2). The loop becomes wide, showing the increase in average coercive field $H_C = (H_2 - H_1)/2$, and its center shifts from the origin, representing the emergence of the EB field defined as $H_{\text{EB}} = (H_1 + H_2)/2$. Importantly, in the vicinity of T_{comp} , the EB is negative at $T > T_{\text{comp}}$ and positive at $T < T_{\text{comp}}$ [see panels (c) and (d) in Fig. 2],

i.e., the EB abruptly changes its sign with crossing T_{comp} . This behavior is analogous to that found recently in ErFeO₃ [9]. Moreover, similar to the observations in ErFeO₃, no cooling-field dependence of EB was detected in NdFeO₃ crystal. In distinct contrast, in SmFeO₃, with low temperature $T_{\text{comp}} = 4.8$ K, we observe a significant cooling-field-dependent EB at temperatures up to 100 K (see Fig. 3). It was found that in an interval between 6 and 100 K the ZFC magnetization loops show the spontaneous EB with negative sign, while the loops measured with the FC ($H_{\text{cool}} = 10$ kOe) regime show the positive EB [see panels 3(c) and 3(d)]. The change in sign of EB from negative to positive with increasing cooling field H_{cool} , shown in Fig. 3(b), well resembles the phenomenon known in some conventional AFM–FM interface systems, such as FeF₂–Fe bilayers, with a specific spin configuration, compatible with positive EB, arising when large enough H_{cool} overcomes the AFM interfacial coupling [23]. It is interesting that Sm orthoferrite shows the cooling-field-induced positive EB, whereas in both Nd and Er orthoferrites only the negative EB occurs at $T > T_{\text{comp}}$. The different behavior may be connected with the fact that in both Nd and Er orthoferrites the weak FM moment of Fe reorients from the *c* axis to the *a* axis at temperatures around 100 K. [See, in Fig. 1(c), the change in magnetization related to the Fe spin reorientation in NdFeO₃.] For this reason, the low-temperature magnetization is not influenced by the magnetic history that happened above

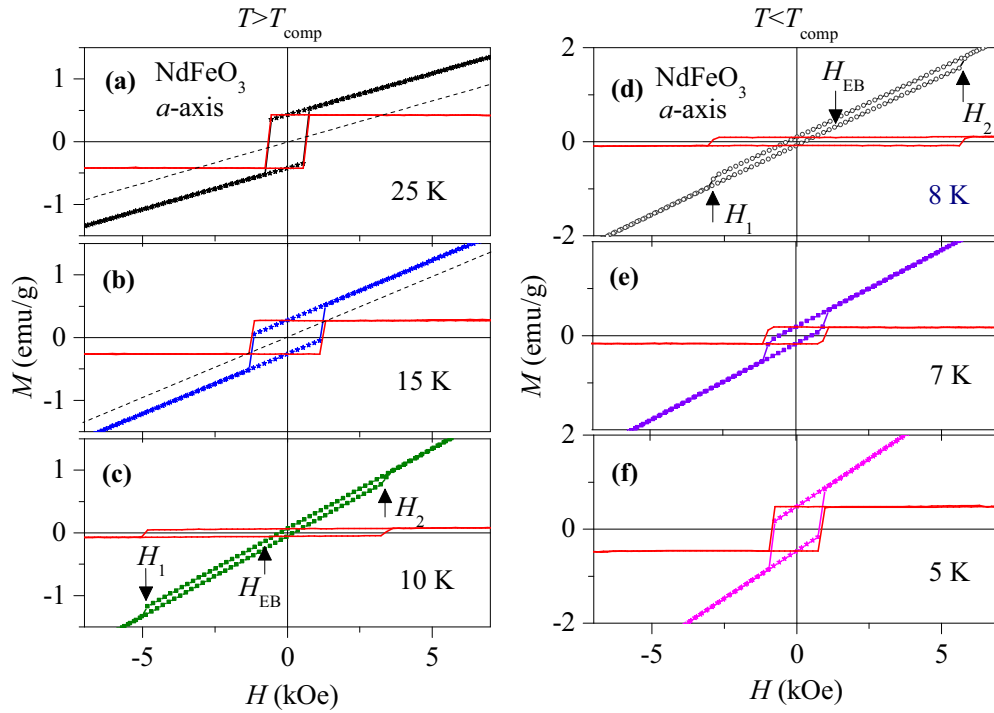


FIG. 2. Magnetization hysteresis loops of NdFeO_3 , in an extended scale, measured between ± 15 kOe and with cooling field 15 kOe along the a axis at temperatures $T > T_{\text{comp}} = 9.2$ K (a, b, c) and at $T < T_{\text{comp}}$ (d, e, f). The dashed lines show the AFM contribution, and the solid lines present the FM contribution to the loops, calculated by extracting the AFM contribution from the original $M(H)$ loops. Arrows indicate the fields of the first and the second magnetization reversals, H_1 and H_2 , respectively, and EB fields, H_{EB} .

the spin-reorientation temperature T_{SR} . In contrast, the weak FM moment of Sm orthoferrite is aligned along the a axis already below $T_{\text{SR}} = 480$ K, and therefore its magnetization

depends on the field-cooling procedure. (Note that the cooling field is applied at 300 K.) Importantly, the ferrimagnetic order in SmFeO_3 is more complex than that of Nd and Er

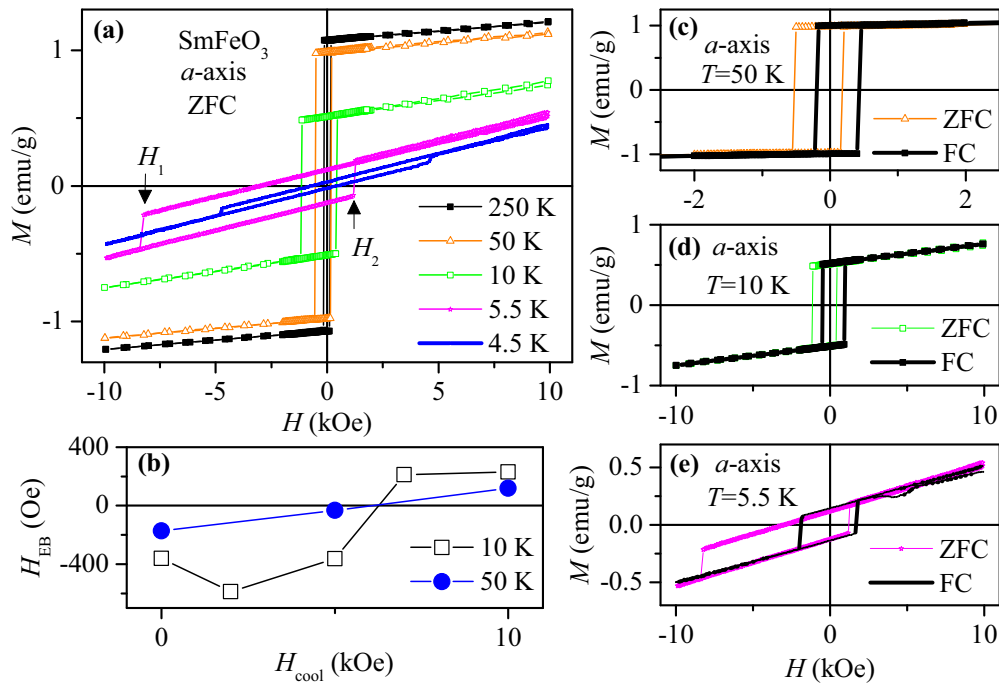


FIG. 3. (a) Magnetization hysteresis loops of SmFeO_3 , measured in ZFC mode along the a axis at various temperatures. (b) Cooling-field dependence of EB field H_{EB} at 10 and 50 K. Hysteresis loops measured along the a axis in both ZFC and FC ($H_{\text{cool}} = 10$ kOe) modes at (c) 50 K, (d) 10 K, and (e) 5.5 K.

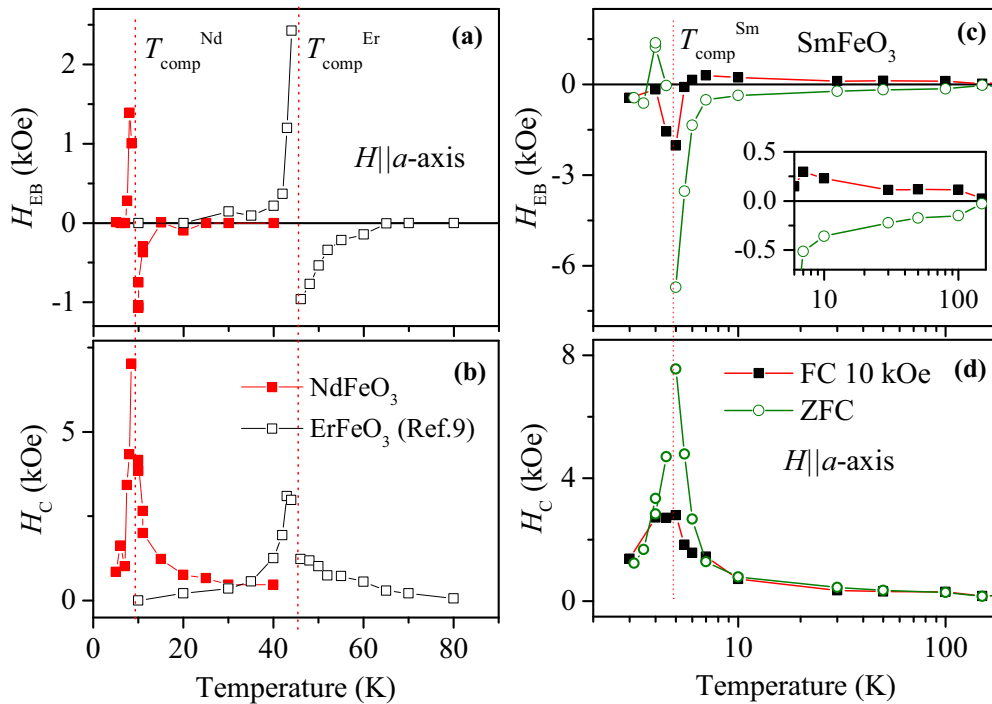


FIG. 4. Temperature dependences of exchange-bias field H_{EB} (a, c) and average coercive field H_C (b, d) of Nd, Sm, and Er orthoferrites. (Data for ErFeO_3 are taken from Ref. [9].) Remarkably, the EB increases on approaching the compensation point T_{comp} and changes sign across T_{comp} . The inset of (c) shows positive and negative H_{EB} of SmFeO_3 corresponding to the FC and ZFC modes, respectively, between 6 and 100 K.

orthoferrites due to the presence of two nonequivalent canted AFM Fe spin pairs. Both nonequivalent Fe and Sm spins were found in SmFeO_3 by the first-principles calculations and confirmed by x-ray magnetic circular dichroism at 360 K [3]. Due to the strong Sm-Fe AFM interaction, two inequivalent Fe and Sm spin orders with antiparallel FM moments along the a axis activate at temperatures just below ~ 135 K [6]. These magnetic orders may compete, depending on the value of applied cooling field H_{cool} , giving rise to the specific spin configurations with the FM moment opposite to applied field, as is required for the positive EB existence [23]. With decreasing T , the larger H_{cool} is required to overcome the AFM Sm-Fe interaction and to observe the positive EB, see Fig. 3(b). Probably, the cooling field of 10 kOe is too small to obtain a positive EB below 6 K around the $T_{\text{comp}}^{\text{Sm}}$, see Figs. 3(e) and 4(c). It should be noted that a very similar EB sign change in SmFeO_3 with decreasing T may be seen in the shifted FC magnetization loops below 6 K, presented in Fig. 2(d) of recent studies (Ref. [10]), although the authors did not declare this issue.

Figure 4 summarizes the temperature dependences of the EB field H_{EB} and of the average coercive field H_C obtained for the Nd and Sm orthoferrites. Data for ErFeO_3 obtained by us previously (Ref. [9]) are also presented for comparison. All of the data demonstrate the universal EB behavior symptomatic for compensated $R\text{FeO}_3$ ferrimagnets, namely, EB appears in the vicinity of the compensation point, increases and diverges on approaching T_{comp} , and changes its sign across T_{comp} . Importantly, the similar EB vs T behavior occurs in different $R\text{FeO}_3$, exhibiting very different both T_{comp} and R -Fe interactions. Further, we show that this universal EB behavior

fairly agrees with likeness in behavior of the net FM moment of compensated $R\text{FeO}_3$ ferrimagnets.

The spontaneous net FM moments M_{FM} , derived from the $M(H)$ loops, are presented as a function of temperature in Fig. 5. The M_{FM} is in fact the remanent FM moment fixed at $H = 0$ after releasing a relatively strong field of ~ 10 kOe, and therefore it remains in the direction of applied field at $T < T_{\text{comp}}$. Both M_{FM} vs T and vs T/T_{comp} (see inset in Fig. 5) dependences show an excellent resemblance in $R\text{FeO}_3$

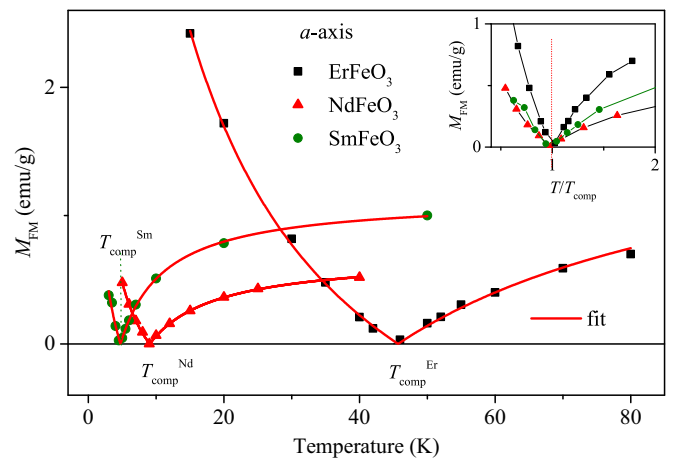


FIG. 5. Temperature dependence of net FM moment M_{FM} derived from the $M(H)$ loops for Nd, Sm, and Er orthoferrites. The inset shows the M_{FM} as a function of reduced temperature T/T_{comp} . The bold lines are the best fit with Eq. (1).

magnetic behavior around T_{comp} . Below the spin-reorientation temperature, the net FM moment of orthoferrites at zero magnetic field could be approximately described within the simple model, taking into account the canted FM moment of Fe spins $M_{\text{FM}}^{\text{Fe}}$, and the opposite paramagnetic moment of R^{3+} , induced by the AFM interaction between Fe^{3+} and R^{3+} spins [24]:

$$M_{\text{FM}} = M_{\text{FM}}^{\text{Fe}} + CH_{\text{int}}/(T - \theta). \quad (1)$$

Here, $C = Ng^2\mu_B^2 S(S+1)/3k_B$ is the Curie constant characterizing the subsystem of free R^{3+} moments with spin S , the H_{int} is an internal exchange field generated by the ordered Fe sublattice and acting on the R spins, and θ is Curie-Weiss temperature linked to the interaction between R^{3+} spins. It was found that Eq. (1) describes well the temperature dependences of M_{FM} for the $R\text{FeO}_3$ fMs presented in Fig. 5 under assumption that the canted moment $M_{\text{FM}}^{\text{Fe}}$ is saturated and unchanged at low temperatures. The bold lines in Fig. 5 are the best fit of Eq. (1) with obtained fitting parameters: $M_{\text{FM}}^{\text{Fe}} = 0.680 \pm 0.006$, 1.14 ± 0.03 , 1.94 ± 0.06 emu/g, $CH_{\text{int}} = -6.8 \pm 0.15$, -7.5 ± 0.5 , -107 ± 6 emu K/g, and $\theta = -0.8 \pm 1$, -1.8 ± 0.3 , -9.4 ± 1 K for Nd, Sm, and Er orthoferrites, respectively. As expected, the FM moment of Fe^{3+} and internal field H_{int} have opposite signs, in accordance with the AFM nature of R -Fe interaction, and they both mutually change sign at T_{comp} . Note that for Nd and Sm orthoferrites, the calculated $M_{\text{FM}}^{\text{Fe}}$ values are close to those observed at 300 K, see Fig. 1(a). Furthermore, the Curie-Weiss temperatures obtained are comparable with the value of $\theta = -1.67$ K reported for SmFeO_3 (Ref. [10]) and with the AFM ordering temperatures of Nd^{3+} ($T_N = 1.05$ K) (Ref. [25]) and Er^{3+} ($T_N = 4.3$ K) (Ref. [26]) in $R\text{FeO}_3$. In the case of NdFeO_3 , using the $S = 1/2$ formalism for Nd^{3+} spin with the value of $g = 1.6$, appropriate here since the ground-state Kramers doublet is separated by 122 K from the first excited doublet [25], we have calculated the Curie constant $C^{\text{Nd}} = 9.68 \times 10^{-4}$ emu K/g Oe and hence the internal exchange field $H_{\text{int}}^{\text{Nd}} = -7$ kOe. It implies that the field of 7 kOe, applied along the a axis, counterbalances the internal field $H_{\text{int}}^{\text{Nd}}$ and therefore completely suppresses the T_{ssw} spin switching transition. Actually, it has been observed for NdFeO_3 that the transition at T_{ssw} becomes much weaker and essentially vanishes at applied field of $H = 5$ kOe (Ref. [5]).

The likeness in both EB and net FM moment behaviors in $R\text{FeO}_3$ ferrites is indicative of the unusual origin of EB, which is rather linked to the AFM interactions between R and Fe ions controlling the field-induced magnetization reversal. One may say that the EB in bulk single-phase $R\text{FeO}_3$ materials

results from the exchange coupling between two internal R and Fe magnetic sublattices, in contrast to the usual EB which requires the presence of the interface between two different magnetic phases. Nevertheless, some principal features of the emergent EB at T_{comp} may be understood in terms of the conventional EB involving a FM/AFM interface, for which, in particular, the field H_{EB} is inversely proportional to the net moment of the soft FM component [11,12]. Similarly, in $R\text{FeO}_3$ ferrimagnets the EB field increases enormously at T_{comp} when the compensated FM moment approaches a zero value, while EB completely disappears far from T_{comp} because the net FM moment becomes too large to be pinned by the AFM R -Fe interaction. Moreover, the EB sign in $R\text{FeO}_3$ ferrites is determined by the mutual orientation of both FM moment and applied magnetic field, in analogy with that in traditional EB systems [23]. It is seen in Fig. 4 that EB is generally negative at $T > T_{\text{comp}}$, when the equilibrium state with parallel FM moment and field is realized, and EB always becomes positive immediately after crossing T_{comp} , when the metastable state with opposite FM moment emerges. The noticed likeness with traditional EB in FM/AFM interfacial systems allows us to presume $R\text{FeO}_3$ as a system composed of two interacting magnetic sublattices, where the R sublattice possesses the pinned FM component and the Fe one plays a role of the strongly anisotropic AFM layer, while the AFM R -Fe interaction is an analog of the interfacial exchange interaction.

III. CONCLUSIONS

In summary, we showed that the field-induced ferromagnetic moment reversal in known compensated ferrimagnets $R\text{FeO}_3$ ($R = \text{Nd, Sm, Er}$) is analogously exchange biased around their compensation temperatures T_{comp} . It appears that, in spite of very different R -Fe interactions, T_{comp} values, and spin-reorientation temperatures in these orthoferrites, the EB field similarly emerges and diverges upon approaching T_{comp} and changes sign with crossing T_{comp} . In addition, SmFeO_3 , with a complicated AFM order caused by the nonequivalent spin configuration, shows EB also at temperatures far above T_{comp} , and its sign alters from negative to positive with increasing cooling field.

ACKNOWLEDGMENTS

This work was partly supported by the Polish NCN through Grant No. 2014/15/B/ST3/03898. E.E.Z. is thankful for support through the Fundamental Research Program funded by the Ministry of Education and Science of Ukraine, Project No. 0117U002360.

- [1] J. A. de Jong, A. V. Kimel, R. V. Pisarev, A. Kirilyuk, and Th. Rasing, *Phys. Rev. B* **84**, 104421 (2011).
 [2] A. V. Kimel, B. A. Ivanov, R. V. Pisarev, P. A. Usachev, A. Kirilyuk, and Th. Rasing, *Nat. Phys.* **5**, 727 (2009).

- [3] J.-H. Lee, Y. K. Jeong, J. H. Park, M.-A. Oak, H. M. Jang, J. Y. Son, and J. F. Scott, *Phys. Rev. Lett.* **107**, 117201 (2011).
 [4] S. Cao, H. Zhao, B. Kang, J. Zhang, and W. Ren, *Sci. Rep.* **4**, 5960 (2014).

- [5] S. J. Yuan, W. Ren, F. Hong, Y. B. Wang, J. C. Zhang, L. Bellaiche, S. X. Cao, and G. Cao, *Phys. Rev. B* **87**, 184405 (2013).
- [6] Y. K. Jeong, J.-H. Lee, S.-J. Ahn, and H. M. Jang, *Solid State Commun.* **152**, 1112 (2012).
- [7] P. D. Kulkarni, A. Thamizhavel, V. C. Rakhecha, A. K. Nigam, P. L. Paulose, S. Ramakrishnan, and A. K. Grover, *Europhys. Lett.* **86**, 47003 (2009).
- [8] K. Yoshii, *Appl. Phys. Lett.* **99**, 142501 (2011).
- [9] I. Fita, A. Wisniewski, R. Puzniak, V. Markovich, and G. Gorodetsky, *Phys. Rev. B* **93**, 184432 (2016).
- [10] X. Wang, S. Gao, X. Yan, Q. Li, J. Zhang, Y. Long, K. Ruan, and X. Li, *Phys. Chem. Chem. Phys.* **20**, 3687 (2018).
- [11] W. H. Meiklejohn and C. P. Bean, *Phys. Rev.* **102**, 1413 (1956); **105**, 904 (1957).
- [12] J. Nogués, J. Sort, V. Langlais, V. Skumryev, S. Suriñach, J. S. Muñoz, and M. D. Baró, *Phys. Rep.* **422**, 65 (2005).
- [13] W. H. Meiklejohn, *J. Appl. Phys.* **33**, 1328 (1962).
- [14] P. J. van der Zaag, A. R. Ball, L. F. Feiner, R. M. Wolf, and P. A. A. van der Heijden, *J. Appl. Phys.* **79**, 5103 (1996).
- [15] Y. Ijiri, T. C. Schulthess, J. A. Borchers, P. J. van der Zaag, and R. W. Erwin, *Phys. Rev. Lett.* **99**, 147201 (2007).
- [16] S. Dong, K. Yamauchi, S. Yunoki, R. Yu, S. Liang, A. Moreo, J.-M. Liu, S. Picozzi, and E. Dagotto, *Phys. Rev. Lett.* **103**, 127201 (2009).
- [17] D. J. Webb, A. F. Marshall, A. M. Toxen, T. H. Geballe, and R. M. White, *IEEE Trans. Magn.* **24**, 2013 (1988).
- [18] G. Gorodetsky and B. Lüthi, *Phys. Rev. B* **2**, 3688 (1970); G. Gorodetsky, L. M. Levinson, S. Shtrikman, D. Treves, and B. M. Wanklyn, *Phys. Rev.* **187**, 637 (1969).
- [19] Z.-P. Li, J. Eisenmenger, C. W. Miller, and I. K. Schuller, *Phys. Rev. Lett.* **96**, 137201 (2006).
- [20] A. Kumar and S. M. Yusuf, *Phys. Rep.* **556**, 1 (2015).
- [21] L. T. Tsymbal, G. N. Kakazei, and Ya. B. Bazaliy, *Phys. Rev. B* **79**, 092414 (2009).
- [22] D. J. Webb, A. F. Marshall, Z. Sun, T. H. Geballe, and R. M. White, *IEEE Trans. Magn.* **24**, 588 (1988).
- [23] J. Nogués, D. Lederman, T. J. Moran, and I. K. Schuller, *Phys. Rev. Lett.* **76**, 4624 (1996).
- [24] A. H. Cooke, D. M. Martin, and M. R. Wells, *J. Phys. C: Solid State Phys.* **7**, 3133 (1974).
- [25] J. Bartolome, E. Palacios, M. D. Kuz'min, F. Bartolome, I. Sosnowska, R. Przeniosło, R. Sonntag, and M. M. Lukina, *Phys. Rev. B* **55**, 11432 (1997).
- [26] W. G. Koehler, E. O. Wollan, and W. K. Wilkinson, *Phys. Rev.* **118**, 58 (1960).